Progress In Electromagnetics Research B, Vol. 26, 23–38, 2010

ADAPTIVE NULLING WITH WEIGHT CONSTRAINTS

R. L. Haupt

Applied Research Laboratory
Pennsylvania State University
P. O. Box 30, State College, PA 16803, USA

Abstract—Adaptive nulling algorithms that minimize the total array output power from the array require constraints on the adaptive weights, otherwise nulls would be placed in the main beam and the desired signal rejected. The concept of cancellation patterns is reviewed and extended to partial adaptive nulling. Cancellation patterns are then extracted from adaptive nulling results with a genetic algorithm and a 32 element dipole array model. The cancellation patterns provide insight into the constraints needed for the successful implementation of a power minimization adaptive algorithm.

1. INTRODUCTION

An adaptive array manipulates the antenna pattern using amplitude and phase weighting of the element signals in order to receive the desired signal entering the main beam while placing nulls in the directions of the interfering signals entering the sidelobes. Most adaptive nulling algorithms require an estimate of the signal correlation matrix in order to find the adapted weights [1]. These algorithms are based upon the Wiener Hopf solution and find the adaptive weights by optimizing a performance measure like signal to noise ratio. Eigenvectors and eigenvalues of the autocorrelation matrix indicate the number, locations, and strengths of the signals incident on the array [2].

The problem with most adaptive algorithms is that they need to accurately know the signal at each element in the array in order to form the estimate of the signal correlation matrix [3]. Errors in the signal path cause corresponding errors in the correlation matrix that result in adaptive weights that do not place the desired nulls in the sidelobes. Consequently, extensive array calibration and compensation schemes

Received 8 July 2010, Accepted 10 September 2010, Scheduled 23 September 2010
Corresponding author: R. L. Haupt (haupt@ieee.org).

are required in order to equalize path lengths and signal strengths at the elements [4].

Digital beamforming offers the best approach to hosting an adaptive nulling algorithm, because all of the weight adjustments are done in software [5]. Although digital beamforming is becoming more widely available [6], most antenna arrays deliver signals to and receive signals from the elements via a corporate feed. T/R modules placed at each element form an active electronically scanned array that electronically steers beams [7]. The T/R modules provide control over the amplitude and phase of the signals at the elements but do not detect the signals at each element. A passive electronically scanned array has phase shifters at each element and little to no amplitude control.

Another approach to adaptive nulling minimizes the total output power of the array [8]. Since setting the amplitudes at each element equal to zero minimizes the output power, amplitude weight constraints are necessary for a practical adaptive antenna system. An alternative to nulling with amplitude weights that preserves the quiescent amplitude taper is phase-only nulling [9]. Even though phase-only nulling cannot zero the amplitude weights, it can set half the elements out of phase with the other half in order to form a null in the middle of the main beam and reject the desired signal. Limiting the phase by using only the least significant bits in the phase shifters has been suggested as a solution to this problem [10]. Another approach, called partial adaptive nulling, limits the nulling of the desired signal by making only a subset of the elements in the array adaptive [11]. This approach limits the damage to the main beam while allowing nulls to be placed in the sidelobes.

Placing a null in an array pattern is equivalent to subtracting a cancellation pattern from the quiescent pattern when the cancellation pattern equals the quiescent pattern at the desired null locations. There are an infinite number of cancellation patterns that can place the null(s). Section 2 presents mathematical representations for the cancellation beam. Section 3 presents techniques for synthesizing patterns with desired nulls (deterministic nulling). Section 4 presents adaptive nulling results for a model that used a genetic algorithm and a full wave electromagnetic model of a 32 element dipole array. The genetic algorithm minimizes the total output power by employing the weight constraints introduced in Section 3. The cancelation pattern for the adaptive nulling results are found by subtracting the quiescent pattern from the adapted pattern. A similar approach is used in Section 5 to find the cancelation pattern for experimental adapted patterns.

2. CANCELLATION PATTERNS

This section establishes the definitions of the quiescent, adapted, and cancellation patterns that are used in this paper. The quiescent pattern of an N-element linear array along the x-axis is defined by its amplitude taper (a_n) and the main beam steered to $\phi = 90°$ as measured from the positive x-axis.

$$QP = \sum_{n=1}^{N} a_n e^{jk(n-1)d\cos\phi} \tag{1}$$

where d is the element spacing and k is the wavenumber. An adaptive array modifies the amplitude and/or phase of the element weights in order to place M nulls in the directions of interference, ϕ_m. The nulled array factor can be written as [12]

$$\begin{aligned} AF &= \sum_{n=1}^{N} w_n e^{jk(n-1)d\cos\phi} \\ &= \sum_{n=1}^{N} a_n e^{jk(n-1)d\cos\phi} - \sum_{m=1}^{M} \gamma_m \sum_{n=1}^{N} a_n e^{jk(n-1)d(\cos\phi-\cos\phi_m)} \\ &= QP + CP \end{aligned} \tag{2}$$

where

γ_m = sidelobe level of the quiescent pattern at ϕ_m.

$w_n = a_n - \sum\limits_{m=1}^{M} \gamma_m c_n e^{-jnkd\cos\phi_m}$ = adapted weights.

c_n = amplitude taper of the cancellation beam.

When $c_n = a_n$, the cancelation pattern is identical to the quiescent pattern. When $c_n = 1.0$, the cancelation pattern is a uniform array factor. For instance, if the array is uniform ($a_n = 1$), then

$$\gamma_m = \frac{\sin(Nkd\cos\phi_m/2)}{N\sin(kd\cos\phi_m/2)} \tag{3}$$

The adaptive weights can also be written as perturbations to the quiescent weights.

$$w_n = a_n (1 - \Delta_n) e^{j\delta_n} \quad 0 \leq \Delta_n \leq 1 \quad \text{and} \quad 0 \leq \delta_n \leq 2\pi \tag{4}$$

where Δ_n and δ_n are the amplitude and phase perturbations from the quiescent weights, respectively. Substituting (4) into (2) and solving for the cancellation pattern yields

$$\begin{aligned} CP &= AF - QP \\ &= \sum_{n=1}^{N} (1-\Delta_n)\, e^{j\delta_n} a_n e^{jk(n-1)d\cos\phi} - \sum_{n=1}^{N} a_n e^{jk(n-1)d\cos\phi} \\ &= \sum_{n=1}^{N} \left(e^{j\delta_n} - \Delta_n e^{j\delta_n} - 1\right) a_n e^{jk(n-1)d\cos\phi} \end{aligned} \tag{5}$$

Thus, the cancellation pattern for any computed or measured adapted pattern is found by simply subtracting the quiescent pattern from the adapted pattern.

If the amplitude and phase of the adapted weights are small (such as when constraints are placed on the adaptive weights), then $e^{j\delta_n} \approx 1 + j\delta_n$ for $\delta_n \ll 1$, and the cancellation pattern is given by

$$\begin{aligned} CP &\approx \sum_{n=1}^{N} \left[1 + j\delta_n - \Delta_n (1 + j\delta_n) - 1\right] a_n e^{jk(n-1)d\cos\phi} \\ &\approx \sum_{n=1}^{N} (j\delta_n - \Delta_n)\, a_n e^{jk(n-1)d\cos\phi} \end{aligned} \tag{6}$$

Phase-only nulling ($\Delta_n = 0$) has a cancelation pattern given by

$$CP \approx \sum_{n=1}^{N} j\delta_n a_n e^{jk(n-1)d\cos\phi} \tag{7}$$

3. NULL SYNTHESIS AND CANCELATION PATTERNS

Null synthesis is an open loop process that derives weights that place nulls in the array factor at known locations. Setting the array factor in (2) equal to zero at M different angles (the size of M depends upon the number of adjustable or adaptive weights)

$$\sum_{n=1}^{N} a_n (1-\Delta_n)\, e^{j\delta_n} e^{jk(n-1)d\cos\phi_m} = 0, \quad m = 1, 2, \ldots, M \tag{8}$$

Writing (8) in matrix form results in

$$Ax = b \tag{9}$$

where

$$A = \begin{bmatrix} a_1 & \cdots & a_N e^{jk(N-1)d\cos\phi_1} \\ \vdots & \ddots & \vdots \\ a_1 & \cdots & a_N e^{jk(N-1)d\cos\phi_M} \end{bmatrix}$$

$$x = \left[(1-\Delta_1)\, e^{j\delta_1} \quad \cdots \quad (1-\Delta_N)\, e^{j\delta_N}\right]^T$$

$$b = [0 \quad \cdots \quad 0]^T$$

The phase term in x requires a nonlinear solution to this equation.

For low sidelobes, only small perturbations to the weights are needed to place nulls. Assuming that $\Delta_n \ll 1$ and $\delta_n \ll 1$results in linearizing (9) with

$$x = [\Delta_1 - j\delta_1 \quad \cdots \quad \Delta_N - j\delta_N]^T$$

$$b = \left[\sum_{n=1}^{N} a_n e^{jk(n-1)d\cos\phi_1} \quad \cdots \quad \sum_{n=1}^{N} a_n e^{jk(n-1)d\cos\phi_M}\right]^T$$

Now, a linear matrix solver finds the weight perturbations needed to place the nulls.

An adaptive array that has $N_a (N_a < N)$ variable weights for placing nulls is known as a partially adaptive array. The weights in (4) for a partially adaptive array are given by

$$w_n = \begin{cases} a_n (1-\Delta_n)\, e^{j\delta_n} & \text{if element } n \text{ is adaptive} \\ a_n & \text{if element } n \text{ is not adaptive} \end{cases} \tag{10}$$

The first examples demonstrating null synthesis assume a fully adaptive array, $N_a = N$. Consider a linear array of 32 isotropic point sources spaced $\lambda/2$ apart. The quiescent array has a 30 dB $\bar{n} = 7$ Taylor taper. Fig. 1 overlays the quiescent pattern, adapted pattern, and cancelation pattern when a null is synthesized at $\phi = 106.25°$. When $c_n = 1$, the patterns in Fig. 1(a) result. The adapted pattern is minimally perturbed near the null, because the beamwidth of the cancelation beam is a minimum. When $c_n = a_n$, the patterns in Fig. 1(b) result. The sidelobes near the synthesized null in the adapted pattern become over 2 dB higher, because the beamwidth of the cancelation beam is wider due to the amplitude taper.

A second example places the same null in the array factor using phase-only nulling with $c_n = a_n$. The cancelation pattern is shown superimposed on the quiescent and adapted patterns in Fig. 2. Note the increased sidelobe in the symmetric location about the main beam ($\phi = 73.75°$). These symmetric sidelobes can only be eliminated using very large phase shifts [13] which cause severe array factor distortions.

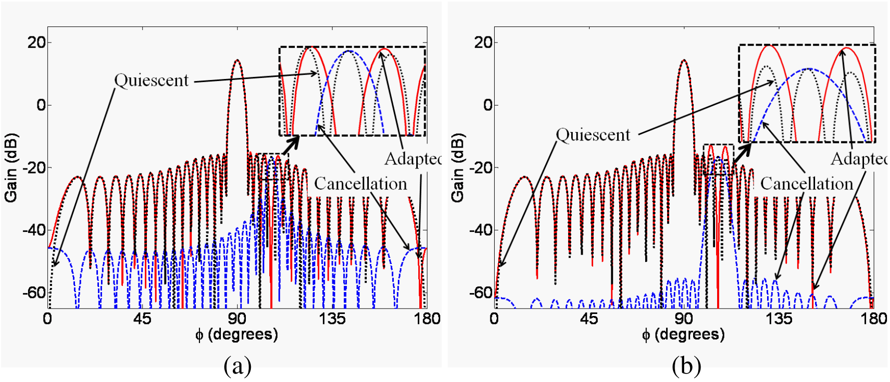

Figure 1. Null placed at $\phi = 106.25°$ in 30 dB $\bar{n} = 7$ Taylor quiescent pattern with cancelation patterns that are (a) uniform $c_n = 1.0$ (b) tapered $c_n = a_n$.

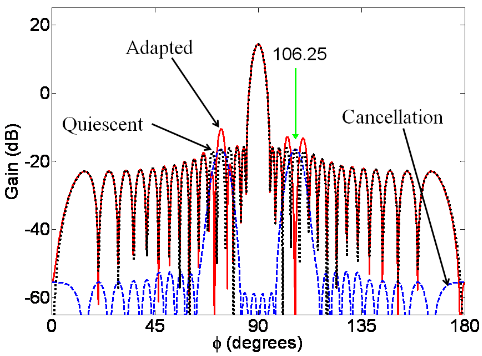

Figure 2. The cancelation pattern (dashed line) superimposed on the quiescent pattern and adapted pattern when a null is placed at $\phi = 106.25°$ using phase weights and $c_n = a_n$.

Figure 3 shows the cancelation patterns associated with placing a null at $\phi = 106.25°$ in the array factor when $N_a = 8$ out of the $N = 32$ elements have adaptive weights. Four different partially adaptive array configurations are considered that have the following adaptive elements:

(a) 1, 2, 3, 4, 29, 30, 31, 32;
(b) 13, 14, 15, 16, 17, 18, 19, 20;
(c) 1, 5, 9, 13, 17, 21, 25, 29;
(d) 2, 8, 13, 16, 18, 23, 24, 30.

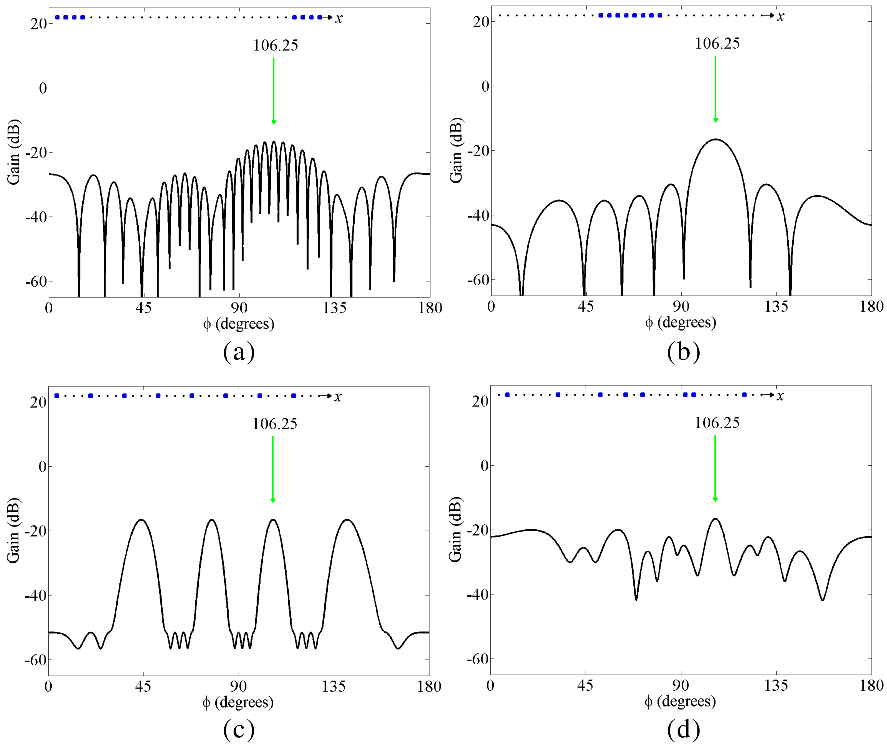

Figure 3. Cancelation patterns for 4 different selections of adaptive elements that place a null at $\phi = 106.25°$. The array at the top of the plots shows a diagram of the linear array along the x-axis. Adaptive elements are indicated by large squares. (a) adaptive elements: 1, 2, 3, 4, 29, 30, 31, 32; (b) adaptive elements: 13, 14, 15, 16, 17, 18, 19, 20; (c) adaptive elements: 1, 5, 9, 13, 17, 21, 25, 29; (d) adaptive elements: 2, 8, 13, 16, 18, 23, 24, 30.

All the configurations have a cancelation pattern peak at $\phi = 106.25°$, but the rest of the cancelation patterns are very different.

The location of the adaptive elements determines the shape of the cancelation pattern which in turn determines the distortion to the adapted pattern. When 4 elements on each end of the array are adaptive, then a very broad but highly oscillatory cancelation pattern main beam results as shown in Fig. 3(a). When 8 adaptive elements are contiguous, then the cancelation beam in Fig. 3(b) results. This cancelation pattern is just an 8 element uniform array factor with its main beam steered to $\phi = 106.25°$. Separating the adaptive elements by regular intervals induces grating lobes in the cancelation pattern as shown in Fig. 3(c). Random spacing of the adaptive elements produces the high sidelobe but narrow main beam cancelation pattern in Fig. 3(d).

4. ADAPTIVE NULLING WITH WEIGHT CONSTRAINTS

Partial adaptive nulling is one way to prevent unwanted main beam nulling when minimizing the total output power. Another way is to put upper bounds on Δ_n and δ_n. Limiting the range of the adaptive weight means that

$$0 \le \Delta_n \le \Delta_{\max} \text{ and } 0 \le \delta_n \le \delta_{\max} \tag{11}$$

Limits are enforced by using the least significant bits of the phase shifter and/or attenuator. For instance, using the 3 least significant bits of a phase shifter with 8 bits and an attenuator with 8 bits ($N_{bits} = 8$) results in $2^3 = 8$ possible adaptive weight settings bounded by

$$0 \le \Delta_n \le 0.0273 \text{ and } 0 \le \delta_n \le 0.0273 \times 2\pi \tag{12}$$

The weight limits need to be large enough to place the nulls but small enough to minimize pattern distortion.

This section looks at adaptive nulling via power minimization with a genetic algorithm on a 32 element array of z-oriented dipoles along the x-axis as shown in Fig. 4. Each dipole is 0.48λlong, and elements

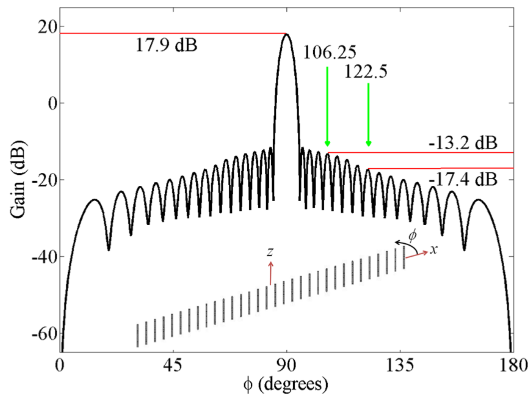

Figure 4. 32 element array of dipoles along the x-axis Quiescent pattern of the 32 element low sidelobe dipole array.

are separated by 0.5λ. FEKO [14] calculates the currents, electric fields, and far field patterns using the multilevel fast multiple method. The output power is calculated by summing the product of the signal weights times the magnitude of the array pattern in the direction of the desired ($\phi = 0°$) and interfering signals.

$$P = \sum_{m=1}^{M} \left| s_m AP\left(\phi_m\right)\right|^2 \tag{13}$$

where

s_m = signal strength;
ϕ_m = signal direction;
AP = antenna pattern calculated by FEKO.

The quiescent array corresponds to a 30 dB $\bar{n} = 7$ Taylor taper. A plot of the quiescent pattern, Q, appears in Fig. 4 with a diagram of the array model.

Limiting the weights is crucial to insuring that the adapted pattern maintains a close relationship to the quiescent pattern. If all 32 elements are adaptive and the phase shifters at each element have 8 bits, then fewer than 8 bits are necessary to guarantee that a null cannot be placed in the main beam. Two 40 dB interference signals are incident upon the array at $\phi = 106.25°$ and $\phi = 122.5°$ while a 0 dB desired signal is incident at 90°. A genetic algorithm finds the voltages at the dipoles that minimize the array output power in (13). Details on using a genetic algorithm for adaptive nulling and the algorithm convergence are found in [15].

Figure 5(a) demonstrates the adaptive nulling capability of the array when 1 out of the 8 bits (1.4°) are used for nulling when all the elements are adaptive. The cancelation beam peaks at the desired null locations fall far short of the quiescent sidelobe levels (dashed line). As a result, adding the cancelation pattern to the quiescent pattern does not place a null in the sidelobes. Increasing the minimum phase to 3 bits (1.4°, 2.8°, 5.6°) allows the adaptive algorithm to generate a cancelation pattern with enough gain to equal the sidelobes at $\phi = 106.25°$ and $\phi = 136.5°$ as shown in Fig. 5(b). The desired nulls become very deep when 4 out of 8 bits (1.4°, 2.8°, 5.6°, 11.3°) are used for adaptive nulling as shown in Fig. 5(c). As with the cancelation patterns for the array factor null synthesis cases, these phase only cancelation patterns have symmetric peaks at the desired null locations. These cancelation patterns do not have low sidelobes. The cancellation patterns have high sidelobes and a main beam peak that points at $\phi = 90°$.

The cancelation pattern peak at $\phi = 90°$ in Fig. 5 is troubling and occurred on all the GA runs attempted. At first, it seemed

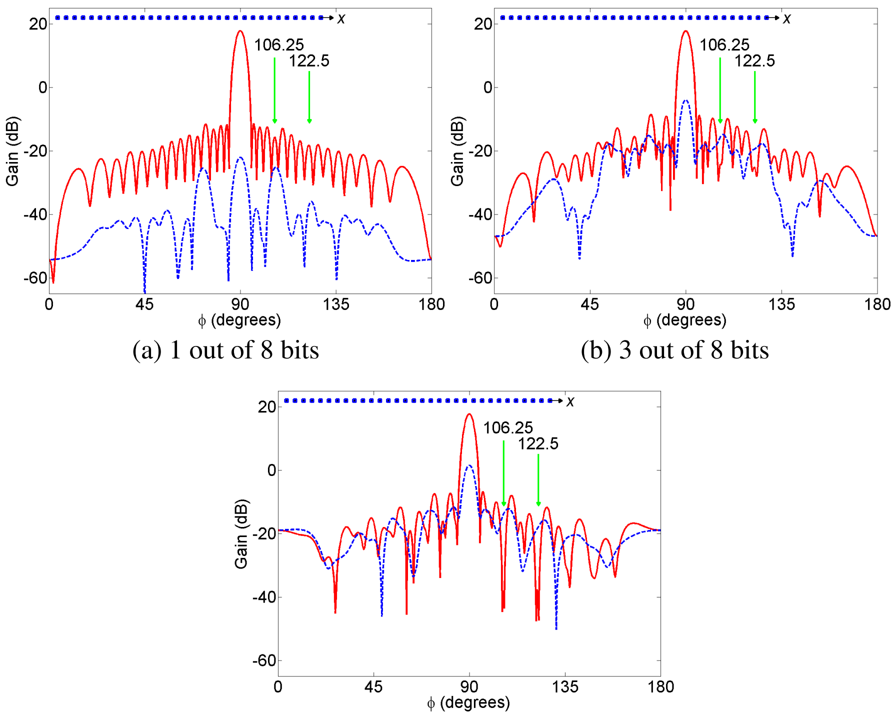

(a) 1 out of 8 bits

(b) 3 out of 8 bits

(c) 4 out of 8 bits

Figure 5. Phase only nulling with the dipole array and limits on the phase quantization. The adapted pattern is the solid line and the cancelation pattern is the dashed line.

logical that the cancelation pattern was trying to null the main beam, because the desired signal was there. However, this peak still occurs when there is no desired signal, and the interference signals are the same. Fig. 6 compares the adaptive phase associated with Fig. 5(b) superimposed on the synthesized phase for a 32 element array of isotropic point sources that is applied to the dipole array. Even though the phases are very similar, the adapted pattern cancelation pattern peak at $\phi = 90°$ is over 36 dB higher than the synthesized cancelation pattern peak, as shown in Fig. 7. The phase in Fig. 6 is antisymmetric about the center of the array, while the adapted phase is not. This antisymmetry reduces the cancelation pattern peak at $\phi = 90°$, because the cancelation beam is an odd function with a zero at $\phi = 90°$. The small peak at $\phi = 90°$ in the synthesized cancelation beam is due to the small phase approximation used in the derivation.

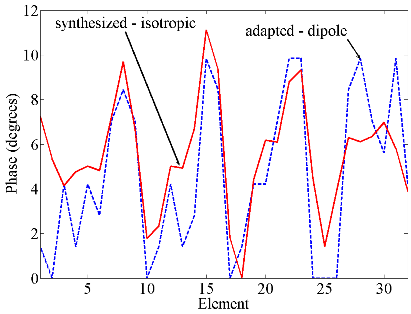

Figure 6. Adaptive phase (phase-only nulling with 3 bits) from 32 element dipole array compared to the synthesized phase of the 32 element array of isotropic point sources.

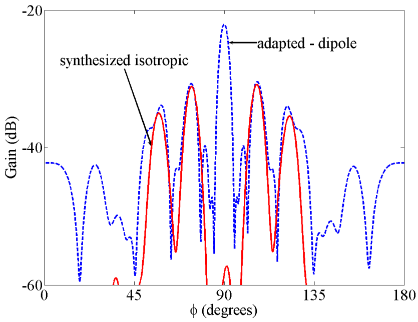

Figure 7. Adaptive cancelation pattern from the 32 element dipole array compared to the synthesized cancelation pattern of the 32 element array of isotropic point sources.

In order to eliminate the cancelation beam peak at $\phi = 90°$, antisymmetry is enforced by adjusting only the first 16 out of 32 phase shifters, while the symmetric 16 elements receive the bitwise complement phase shift. Thus, using 4 out of 8 bits to perform the adaptive nulling, if element 1's phase shifter receives the 8-bit word

$$[* \quad * \quad * \quad * \quad 1 \quad 0 \quad 1 \quad 0]$$

then element 32 receives this 8-bit word

$$[\# \quad \# \quad \# \quad \# \quad 0 \quad 1 \quad 0 \quad 1]$$

Figure 8 shows the adapted pattern when interference at $\phi = 106.25°$ and $122.5°$. The adapted phase weights appear in Fig. 9. This phase-only adaptive algorithm used 4 out of 8 bits with half the elements on one side receiving the bitwise complement of the phase shift received by its symmetric counterpart on the other side. The cancelation pattern in this case has a null at $\phi = 90°$ unlike the result shown in Fig. 5(c) when no symmetry constraint was place on the adaptive phase shifts. Although the cancelation beam has a minimum at $\phi = 90°$, it still has peaks that lie inside the main beam, so the main beam will still receive some distortion.

As seen in the previous section, the location of the adaptive elements in a partially adaptive array determines the shape and gain of the cancelation pattern. Fig. 10 shows the adapted and cancelation patterns for the 32 element dipole array when elements 1, 2, 3, 4, 29, 30, 31, and 32 are adaptive for both phase-only and amplitude and

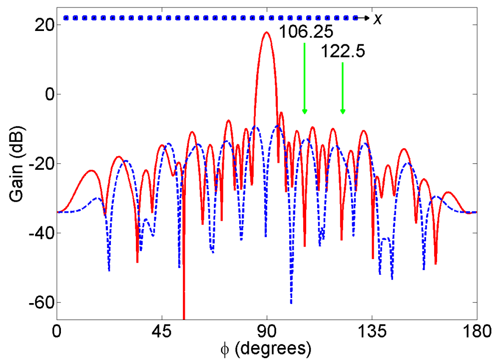

Figure 8. Adapted pattern with interference at $\phi = 106.25°$ and 122.5° and superimposed on the quiescent pattern. Symmetric elements receive bitwise complements of the 4 out of 8 adaptive phase bits in order to minimize the cancelation pattern peak at $\phi = 90°$. The adapted pattern is the solid line and the cancelation pattern is the dashed line.

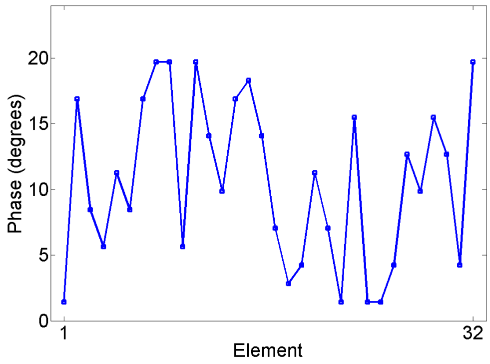

Figure 9. Adapted weights for Fig. 8.

phase adaptive nulling. Since no limits were placed on the element weights, the distortion to the adapted pattern is significant.

The previous example shows that partial adaptive nulling can produce unwanted pattern distortion. This distortion can be controlled by placing limits on the adaptive weights or using fewer adaptive elements. Fig. 11 repeats the previous case but limits the maximum phase shift at the adaptive elements to 90°. These limits result in much less distortion to the adapted pattern while still placing the desired nulls. Fig. 12 shows results when the center 8 elements are adapted and the maximum phase shift at the adaptive elements to 45°. The cancelation pattern in Fig. 12 is very different than the one in Fig. 11 and causes much different distortion to the adapted patterns.

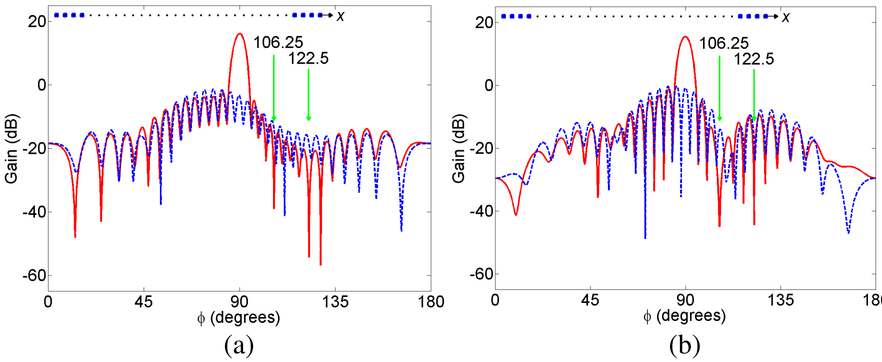

Figure 10. Adapted, quiescent, and cancelation patterns for the 32 element dipole array when elements 1, 2, 3, 4, 29, 30, 31, and 32 are adaptive (a) phase-only (b) amplitude and phase. The adapted pattern is the solid line and the cancelation pattern is the dashed line.

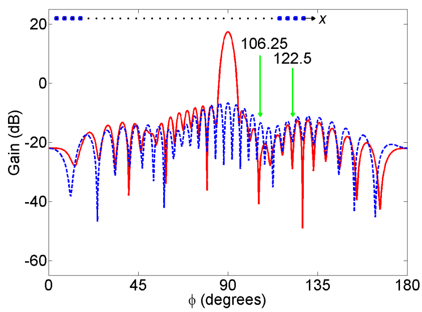

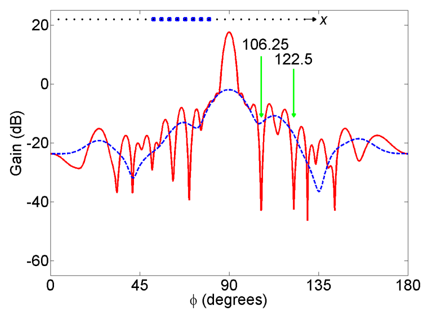

Figure 11. Results for the case in Fig. 10(a) when the adapted phase is limited to 90°. The adapted pattern is the solid line and the cancelation pattern is the dashed line.

Figure 12. Adapted and cancellation patterns of the 32 element dipole array when the center 8 elements were adaptive with a maximum 45 deg phase shift. The adapted pattern is the solid line and the cancellation pattern is the dashed line.

Figure 13 has the adapted pattern with its cancelation pattern when 4 elements are adaptive: 1, 2, 31, 32 with 8 bits of phase. The nulls are placed in the desired directions by a very broad cancelation pattern. It intersects and nulls the quiescent pattern at $\phi = 106.25°$ and $\phi = 122.5°$. The same case for phase-only nulling appears in Fig. 14. Phase-only nulling cause considerably more pattern distortion. Low amplitude weights at the edge elements limit the possible pattern distortion by the cancelation beam.

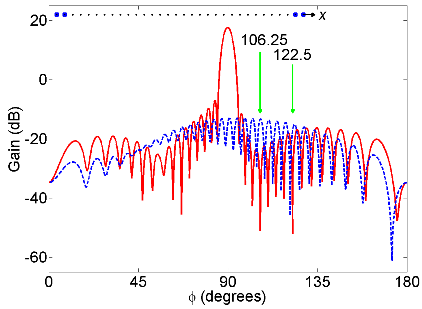

Figure 13. Amplitude and phase adaptive nulling using 4 edge elements. The adapted pattern is the solid line and the cancelation pattern is the dashed line.

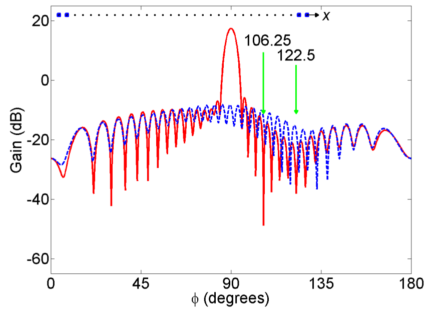

Figure 14. Phase-only adaptive nulling using 4 edge elements. The adapted pattern is the solid line and the cancelation pattern is the dashed line.

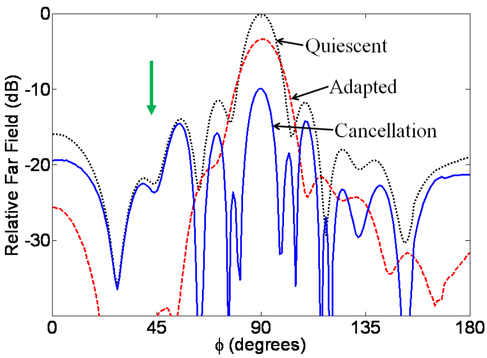

Figure 15. Plots of the experimental quiescent and adapted patterns for a null at 45°. The plot of the cancelation pattern is the difference between the adapted and quiescent patterns.

5. CANCELATION PATTERNS FROM EXPERIMENTAL RESULTS

The cancelation beam can be extracted from experimental results as well. In [15], experimental results for an amplitude-only adaptive 8 element array are presented where elements 1, 2, 7, and 8 are adaptive. The null is adaptively formed at $\phi = 42°$ as shown in Fig. 15. If the quiescent pattern is subtracted from the adapted pattern, then the cancelation beam in Fig. 15 results. Since the weights are amplitude-only, there is no way to reduce the peak of the cancelation beam at $\phi = 90°$ and an over 3 dB main beam reduction in the adapted pattern results.

6. CONCLUSIONS

Adaptive nulling via output power minimization requires constraints on the adaptive weights in order to prevent inadvertent nulling of the desired signal entering the main beam. This paper presented two types of weight constraints: 1) limits on the weights and 2) partial adaptive nulling. Both approaches were analyzed using cancelation patterns in order to understand pattern distortions and nulling capability. The cancelation patterns were found analytically for the arrays of isotropic point sources and numerically for the dipole arrays. Increasing the number of adaptive elements and/or increasing the range of the adaptive weights causes more pattern distortion.

The cancelation pattern for experimental adaptive arrays can be found using the same approach used for the dipole array in this paper. The dipole array in this paper did not take into account reflections from the elements, environmental scattering, or component errors, but experimental results would.

Placing constraints on the adaptive process helps a random search algorithm like the GA, but also simplifies the optimization enough that a local optimizer might work as well.

Finally, finding a way to eliminate the main lobe of the cancelation pattern at $\phi = 90°$ would be helpful. In other words, can the GA be nudged into considering only solutions that have a cancelation pattern with a reduced level at $\phi = 90°$? Making the phase antisymmetric about the center of the array puts a null in the cancelation pattern at $\phi = 90°$ but the lobes next to that null disturb the main beam and reduce the gain.

REFERENCES

1. Gross, F. B., *Smart Antennas for Wireless Communications: With MATLAB*, McGraw-Hill, New York, 2005.
2. Compton, R. T., *Adaptive Antennas: Concepts and Performance*: Prentice-Hall, Philadelphia, Pa., 1987.
3. Monzingo, R. A., R. L. Haupt, and T. W. Miller, *Introduction to Adaptive Arrays*, NC SciTech Publishing, Raleigh, 2010.
4. Tyler, N., B. Allen, and H. Aghvami, "Adaptive antennas: The calibration problem," *IEEE Comm. Mag.*, Vol. 42, No. 12, 114–122, 2004.
5. Steyskal, H., "Digital beamforming antennas: An introduction," *Microwave Journal*, Vol. 30, No. 2, 1–124, 1987.
6. Brookner, E., "Now: Phased-array radars: Past, astounding breakthroughs and future trends," *Microwave Journal*, Vol. 51, No. 1, 31–48, 2008.
7. Frank, J. and J. D. Richards, "Phased array radar antennas," *Radar Handbook*, M. I. Skolnik, Editor, 13.1–13.74, McGraw Hill, New York, 2008.
8. Haupt, R. L. and H. L. Southall, "Experimental adaptive nulling with a genetic algorithm," *Microwave Journal*, Vol. 42, No. 1, 78–89, 1999.
9. Baird, C. A. and G. G. Rassweiler, "Adaptive sidelobe nulling using digitally controlled phase-shifters," *IEEE Transactions on Antennas and Propagation*, Vol. 24, No. 5, 638–649, 1976.
10. Haupt, R. L., "Phase-only adaptive nulling with a genetic algorithm," *IEEE Transactions on Antennas and Propagation*, Vol. 45, No. 6, 1009–1015, 1997.
11. Morgan, D., "Partially adaptive array techniques," *IEEE Transactions on Antennas and Propagation*, Vol. 26, No. 6, 823–833, 1978.
12. Steyskal, H., R. Shore, and R. Haupt, "Methods for null control and their effects on the radiation pattern," *IEEE Transactions on Antennas and Propagation*, Vol. 34, No. 3, 404–409, 1986.
13. Shore, R., "Nulling a symmetric pattern location with phase-only weight control," *IEEE Transactions on Antennas and Propagation*, Vol. 32, No. 5, 530–533, 1984.
14. FEKO Suite 5.4, EM Software and Systems (www.feko.info), 2008.
15. Haupt, R. L., *Antenna Arrays: A Computational Approach*, Wiley, New York, 2010.